molecular pharmaceutics

Article

pubs.acs.org/molecularpharmaceutics

Polymeric Micelles as Carriers for Nerve-Highlighting Fluorescent Probe Delivery

Kayla M. Hackman,[†,‡] Bhuvana Shyam Doddapaneni,[‡,§] Connor W. Barth,[†] Igor H. Wierzbicki,[§] Adam W. G. Alani,[§] and Summer L. Gibbs*[,†,∥,⊥]

[†]Biomedical Engineering Department, [∥]Knight Cancer Institute, and [⊥]OHSU Center for Spatial Systems Biomedicine, Oregon Health & Science University, Portland, Oregon 97201, United States

[§]Pharmaceutical Sciences Division, College of Pharmacy, Oregon State University, 2730 SW Moody Avenue, CL5CP Portland, Oregon 97201, United States

ABSTRACT: Nerve damage during surgery is a common morbidity experienced by patients that leaves them with chronic pain and/or loss of function. Currently, no clinically approved imaging technique exists to enhance nerve visualization in the operating room. Fluorescence image-guided surgery has gained in popularity and clinical acceptance over the past decade with a handful of imaging systems approved for clinical use. However, contrast agent development to complement these fluorescence-imaging systems has lagged behind with all currently approved fluorescent agents providing untargeted blood pool information. Nerve-specific fluorophores are known, however translations of these agents to the clinic has been complicated by their lipophilic nature, which necessitates specialized formulation strategies for successful systemic administration. To date the known nerve-specific fluorophores have only been demonstrated preclinically due to the necessity of a dimethyl sulfoxide containing formulation for solubilization. In the current study, a polymeric micellar (PM) formulation strategy was developed for a representative nerve-specific fluorophore from the distyrylbenzene family, BMB. The PM formulation strategy was able to solubilize BMB and demonstrated improved nerve-specific accumulation and fluorescence intensity when the same fluorophore dose was administered to mice utilizing the previous formulation strategy. The success of the PM formulation strategy will be important for moving toward clinical translation of these novel nerve-specific probes as it is nontoxic and biodegradable and has the potential to decrease the necessary dose for imaging while also improving the safety profile.

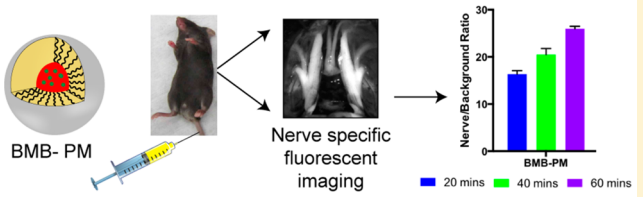

KEYWORDS: *image-guided surgery, nerve-specific fluorescence, polymeric micelle, small molecule formulation*

INTRODUCTION

Nerve damage following surgery is a continued morbidity experienced by up to 600,000 patients annually in the United States alone.[1] Currently, no clinically approved method exists to enhance nerve visualization in the surgical suite. Fluorescence image-guided surgery has the potential to improve nerve identification and visualization in the operating room as interest in fluorescence image-guided surgery has significantly increased in the past decade. Currently, there are numerous fluorescence image-guided surgery systems in clinical trial or approved for clinical use including an FDA approved fluorescence channel in the da Vinci surgical robot manufactured by Intuitive Surgical.[2−9] However, FDA approved fluorescent contrast agents are limited and the current FDA approved agents are not targeted, but rather act as blood pool agents and do not provide specific fluorescent contrast in nerve tissue.[7]

A limited number of fluorescent contrast agents exist that stain nerve tissue *in vivo*, with varying degrees of nerve-specificity and nerve signal to background ratio reported. Design and development of nerve-specific fluorescent probes is challenging, as the blood nerve barrier (BNB) is a tight junction similar to the blood brain barrier (BBB) where only small molecules less than 500 Da can pass freely. Additionally, fluorophores must also have a logarithmic distribution coefficient (Log *D* at pH 7.4) between 0.5 and 3 to optimally partition from the blood into the nerves.[10] There are currently seven known classes of fluorophores that have been shown to have either nerve or brain specificity when administered systemically, which include nerve-specific peptides and six small molecule fluorophore scaffolds. The nerve-specific peptides are a targeting sequence that largely binds to the epineurium with minimal binding to the endoneurium due to their large size.[11] Nerve-specific contrast is generated using this targeting sequence by conjugating a fluorophore of interest, however fluorescence is only seen on the periphery of nerve tissue diminishing signal to background ratio. Three of the small molecule fluorophores reported to have myelin specificity, including stilbene, coumarin, and tricarbocyanine fluorophores, have only demonstrated specific signal in brain tissue and have not shown nerve-specific fluorescence following systemic administration.[12−14] The small molecule styrylpyridinium fluorophores have been demonstrated to partition into the

Received: July 23, 2015
Revised: September 24, 2015
Accepted: October 20, 2015
Published: October 20, 2015

DOI: 10.1021/acs.molpharmaceut.5b00582
Mol. Pharmaceutics 2015, 12, 4386−4394

dorsal nerve root and trigeminal ganglia following systemic administration, but due to the large size of these fluorophores they do not highlight all nerve tissue following systemic administration.[15]

To date only two small molecule fluorophore scaffolds have been found to penetrate the BNB and highlight all nerve tissue following systemic administration, which include the distyrylbenzene (DSB) fluorophores and two select oxazine fluorophores.[10,16,17] A library of DSB fluorophore has been previously synthesized and utilized to determine the structure activity relationship of this fluorophore scaffold for nerve specificity (Figure 1A).[16] In the current work, 4,4′-[(2-methoxy-1,4-phenylene)-di(1*E*)-2,1-ethenediyl]bis-benzenamine (BMB), a representative DSB fluorophore, was selected for further study. BMB is a small molecule with a molecular weight of 342.4 Da, Log *D* of 4.8, and excitation and emission wavelengths of 393 and 503 nm, respectively (Figure 1B).[10] In addition, BMB has an aqueous solubility of 1 μg/mL,[18] necessitating a drug delivery system for clinically relevant concentration administration *in vivo*. Initial studies were performed with a cosolvent formulation of 10% dimethyl sulfoxide (DMSO), 5% Cremophor EL, 65% serum, and 20% HEPES buffer to solubilize BMB for intravenous (iv) administration, where nerve-specific fluorescence was demonstrated.[10] However, the cosolvent formulation is not ideal for clinical translation as it is stable at room temperature for less than 30 min, and it requires the use of DMSO and Cremophor EL, which will hamper future clinical translation due to vehicle toxicity issues. Thus, moving forward a clinically relevant formulation strategy is necessary to fully utilize these derivatives. In the work presented herein a polymeric micellar (PM) formulation strategy has been developed that enhances nerve to muscle ratio over the previously used cosolvent formulation for improved visualization during nerve-sparing surgical procedures.

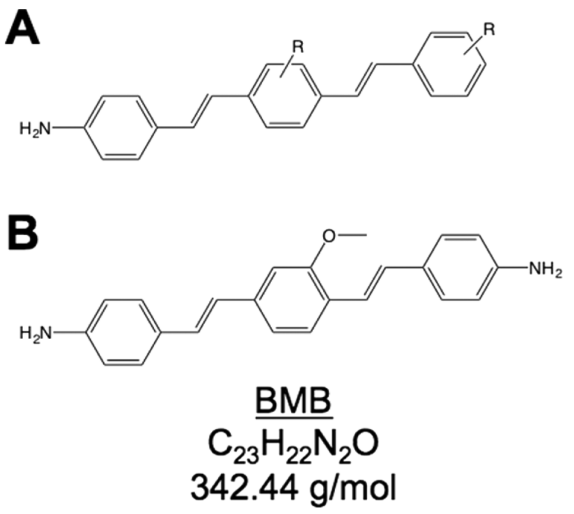

Figure 1. DSB and BMB structure. (A) The DSB fluorophore scaffold has been investigated for nerve-specificity with fluorophores of the para-configuration showing the highest nerve-specific accumulation.[16] (B) BMB is an example of a para-configuration of DSB and was utilized in the current study.

PM are an excellent drug delivery platform for sparingly soluble compounds. PM are nanoscale colloidal dispersions with particle size between 15 and 100 nm.[19−22] The building units for PM are amphiphilic block copolymers (i.e., polymers consisting of a hydrophilic segment and a hydrophilic segment) that self-assemble in aqueous environments into spherical structures (micelles) at concentrations equal to or above critical micelle concentration.[20] The core of these spherical structures is hydrophobic while the shell is hydrophilic.[23] Sparingly soluble compounds, like BMB, tend to partition into the hydrophobic core of the micelles driven by the hydrophobic interactions between the compound and the polymer hydrophobic segments.[24] Such interactions can significantly increase the water solubility of sparingly soluble small molecules and utilize the core as a depot for these compounds.[21,25] The hydrophilic shell is a physical barrier that prevents micelle aggregation and minimizes micelle−protein interaction (opsonization). Therefore, the shell contributes toward the increased stability, which can then translate into longer blood circulation times for the formulated compound. One of the most common amphiphilic block copolymers that is utilized for PM is methoxy poly(ethylene glycol)-*block*-poly(D,L-lactic acid) (PEG-*b*-PLA) due to its safety, biocompatibility, and biodegradability. Genexol, a PM formulation of paclitaxel encapsulated in PEG-*b*-PLA, is currently in phase II clinical trials for the treatment of advanced non-small cell lung cancer.[26] In this work PEG-*b*-PLA PM has been formulated for the delivery of the BMB fluorophore and compared to the previous cosolvent formulation in *ex vivo* and *in vivo* murine models to evaluate PEG-*b*-PLA PM formulated BMB for nerve-specific imaging capability and feasibility for clinical translation for fluorescence image-guided surgery.

EXPERIMENTAL SECTION

Materials. Amphiphilic block copolymer PEG(2000)-*b*-PLA(1800) (M_n = 3800 Da, MW = 4100, and PI = 1.12) was purchased from Advanced Polymer Materials Inc. (Montreal, Canada). Human umbilical vein endothelial cells (HUVEC) and endothelial growth medium 2 were purchased from PromoCell (Heidelberg, Germany). Cells were cultured as per the manufacturer's instructions, and experiments were performed between passages 2 and 6. Abelson murine leukemia virus transformed macrophage cells (RAW 264.7) were purchased from American Type Culture Collection (Manassas, VA). Cell culture supplies including Dulbecco's modified Eagle medium (DMEM), fetal bovine serum (FBS), trypsin EDTA, and penicillin/streptomycin were purchased from VWR (Radnor, PA). CellTiter-Blue Cell Viability Assay kit was obtained from Promega Inc. (Madison, WI). All other reagents were of analytical grade and were purchased from VWR International, LLC (Radnor, PA), or Fisher Scientific Inc. (Fairlawn, NJ) unless stated otherwise below.

Micelle Encapsulation of Nerve-Specific Fluorophore and Release Kinetics. BMB loaded PM were prepared by the solvent casting method.[25] Briefly 2 mg of BMB and 15 mg of PEG-*b*-PLA were dissolved in 0.5 mL of acetonitrile, which was evaporated under reduced pressure to form a thin dye distributed polymeric film. Micelles were obtained by rehydration of the film with 0.5 mL of deionized water. The BMB loading in the micelles was quantified using liquid chromatography mass spectroscopy (LCMS) analysis (Agilent, Santa Clara, CA) as follows. Standard curves for the BMB were obtained using analog signal data from the diode array detector (DAD) at 400 nm to calculate the area under the curve of the identified BMB peak, confirmed by mass to charge ratio from the MS. Briefly, varied concentrations of BMB (10 μL) were injected onto a Poroshell C18 column (Agilent) and separated using a linear gradient from 30% acetonitrile and 70% water to 100% acetonitrile and 0% water

DOI: 10.1021/acs.molpharmaceut.5b00582
Mol. Pharmaceutics 2015, 12, 4386−4394

over 8 min, where BMB had a retention time of 7 min. All water and acetonitrile contained 0.1% formic acid. The standard curve was used to convert area under the curve measurements from the DAD into corresponding BMB concentrations. All concentration quantification measurements were performed in triplicate. BMB-PM size was quantified by dynamic light scattering (DLS) using a Malvern Nano ZS (Malvern Instruments Inc., U.K.). Triplicate samples were prepared for DLS by diluting the micelles 20-fold in DI water to a final concentration of the polymer at 0.1 mg/mL. DLS measurements were collected after equilibration of the micelles in DI water for 2 min.

Freshly prepared BMB-PM samples of 2.5 mL (2 mg/mL) were loaded into a Slide-A-Lyzer (Thermo Scientific Inc.) 3 mL dialysis cassette with a MWCO of 7000 g/mol. This MWCO was chosen to enable the free fluorophore along with the unassociated polymer molecules to diffuse freely out of the cassette and thereby ensure sink conditions. Three cassettes were used in each experiment. The cassettes were placed in 2.5 L of 10 mM phosphate buffer at pH 7.4, which was changed every 3 h to ensure sink conditions, and the temperature was maintained at 37 °C. The sampling time intervals were 0, 0.5, 1, 2, 3, 6, 9, 12, 24, 48, and 72 h. A sample of 100 μL at each time point was withdrawn, and the cassette was replenished with an equal volume of buffer. Samples were analyzed by LCMS for BMB content as described above to quantify free BMB concentration at each time point. The BMB release data from PM was curve-fitted using a two-phase exponential association equation indicative of diffusion and micelle dissociation based fluorophore release. The time required to release 50% of the drug ($t_{1/2}$) in two phases, rapid and sustained, and the goodness of fit (R^2) values of three replicates are presented. The curve fitting analysis was performed with GraphPad Prism version 5.04 for Windows, (GraphPad Software, San Diego, CA).

Cell Viability Studies. HUVEC and RAW 264.7 cell viability in the presence of different concentrations of the BMB-PM solutions was evaluated. HUVEC cells were seeded at the density of 5,000 cells/well in 96-well flat bottom cell culture plates and allowed to attach for 48 h at 37 °C. RAW 264.7 cells were seeded, at 10,000 cells/well in a 96-well flat bottom cell culture plates, and allowed to attach for 24 h at 5% CO_2 maintained at 37 °C. After incubation, cells were treated with different concentrations (10 pM to 100 μM) of BMB-PM or phosphate buffed saline (PBS) as control. Cell viability was determined after 48 h of treatment using 20 μL of CellTiter-Blue followed by 1 h of incubation at 37 °C and evaluated for fluorescence at 560_{Ex}/590_{Em}. All measurements were performed in quadruplicate. The compiled data is presented as mean cell viability ± standard deviation (SD). Significant differences between treatment group means was evaluated using one-way analysis of variance (one-way ANOVA) combined with Dunnette's post-test analysis, where all columns were compared to the PBS, with a threshold value (p-value = 0.05). The analysis was performed using GraphPad Prism.

Animals. Approval for all animals used in this study was obtained from the Institutional Animal Care and Use Committee (IACUC) at Oregon Health and Science University (OHSU). Male CD-1 mice weighing 22−24 g were purchased from Charles River Laboratories (Wilmington, MA). Prior to surgery, mice were anesthetized with an intraperitoneal (ip) injection of a mixture of 100 mg/kg ketamine and 10 mg/kg xylazine (Patterson Veterinary, Devens, MA). All surgeries were terminal, and exposed nerve tissues were resected for further analysis by fluorescence microscopy.

Intraoperative Fluorescence Imaging System. A custom-built real-time fluorescence imaging system was used to collect the murine *in vivo* color and nerve-specific fluorescence images. The fluorescence imaging system consisted of a QImaging EXi Blue monochrome camera (Surrey, British Columbia, Canada) for fluorescence detection with a removable Bayer filter to collect coregistered color and fluorescence images. A PhotoFluor II (89 North, Burlington, VT) was focused onto the surgical field using a liquid light guide for white light illumination and was filtered for BMB excitation with a 405 ± 20 nm bandpass excitation filter. The emitted light was filtered with a 550 ± 25 nm bandpass emission filter for fluorescence image collection. All filters and beam splitters were from Chroma Technology (Bellows Falls, VT). All fluorescence images were collected using 50 ms exposure time and displayed with equal normalization for quantitative comparison.

Murine Nerve Imaging. BMB dose and biodistribution were previously optimized for mouse studies and utilized herein.[10] BMB (BMB-PM or BMB in the cosolvent) was administered at 0.5 mg/kg iv via tail vein to mice (n = 3/group; 5 groups) 4 h prior to surgical exposure and imaging of the brachial plexus, sciatic nerve, trigeminal ganglia, and optic nerves, as well as the surrounding muscle and adipose tissues. The injection volume in mice varied between 100 and 200 μL. Mice were administered BMB-PM or BMB in the cosolvent formulation as treatments, and as controls they were treated with blank PM or cosolvent without BMB (blank cosolvent) or left untreated.[10,16] BMB containing formulations were assessed for nerve signal to background ratio while the BMB negative formulations including untreated mice were used to determine autofluorescence in the nerve, muscle, and adipose tissues. Region of interest analysis was performed at each nerve site to determine the nerve to muscle ratio (N/M) as well as the nerve to adipose ratio (N/A). The mean N/M and N/A ratios for the brachial plexus, sciatic, trigeminal ganglia and optic nerves were calculated from six nerves for each nerve site (2 per mouse) as well as surrounding areas of muscle and adipose tissue for each site.

***Ex Vivo* Fluorescence Microscopy on Resected Nerve Tissues.** Following completion of imaging experiments, the sciatic and brachial plexus nerves from mice (n = 3/group; 5 groups) were harvested, fixed with 2% paraformaldehyde (PFA) for 12 h, snap frozen in optimal cutting temperature (OCT) compound with liquid nitrogen, and stored at −80 °C for *ex vivo* studies. Cryosections were cut at 10 μm onto Superfrost Plus slides (Fisherbrand, Fisher Scientific), mounted with Fluoromount-G (Southern Biotech, Birmingham, AL) and coverslipped prior to microscopy. Images were acquired on an Axio Observer inverted fluorescence microscope (Zeiss, Thornwood, NY) at 20× magnification. A Photofluor II was used for phase contrast images as well as filtered using a 405 ± 20 nm bandpass excitation filter for BMB excitation. Images were collected using an Axiocam 506 camera (Zeiss) where a 550 ± 25 nm bandpass emission filter was used for fluorescence image collection. All images were collected at 1000 ms exposure time and displayed with equal normalization. A group of 10 representative regions of nerve and background were analyzed for each brachial plexus and sciatic nerve image to calculate the nerve to background ratio and standard deviation for each administration group.

***Ex Vivo* Nerve-Specific BMB Staining.** *Ex vivo* nerve-specific BMB staining was completed as previously reported,[10,16] and is described briefly as follows. Brachial plexus and sciatic nerve tissue from untreated mice were collected, fixed with 2% PFA for 12 h, and then snap frozen in OCT with liquid nitrogen.

DOI: 10.1021/acs.molpharmaceut.5b00582
Mol. Pharmaceutics 2015, 12, 4386−4394

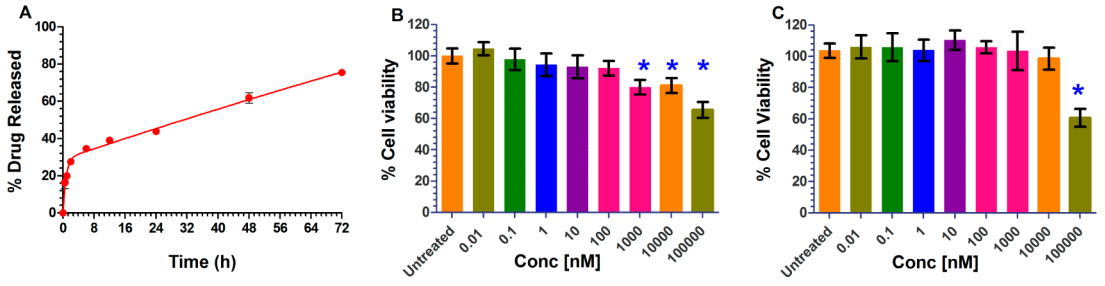

Figure 2. Release kinetics and effect on cell viability. (A) Release kinetics of the BMB from PM measured over 72 h (n = 3). BMB micelle toxicity was assessed using CellTiter-Blue assay for concentrations of BMB ranging from 10 pM to 100 μM in (B) HUVEC and (C) RAW 264.7 cells.

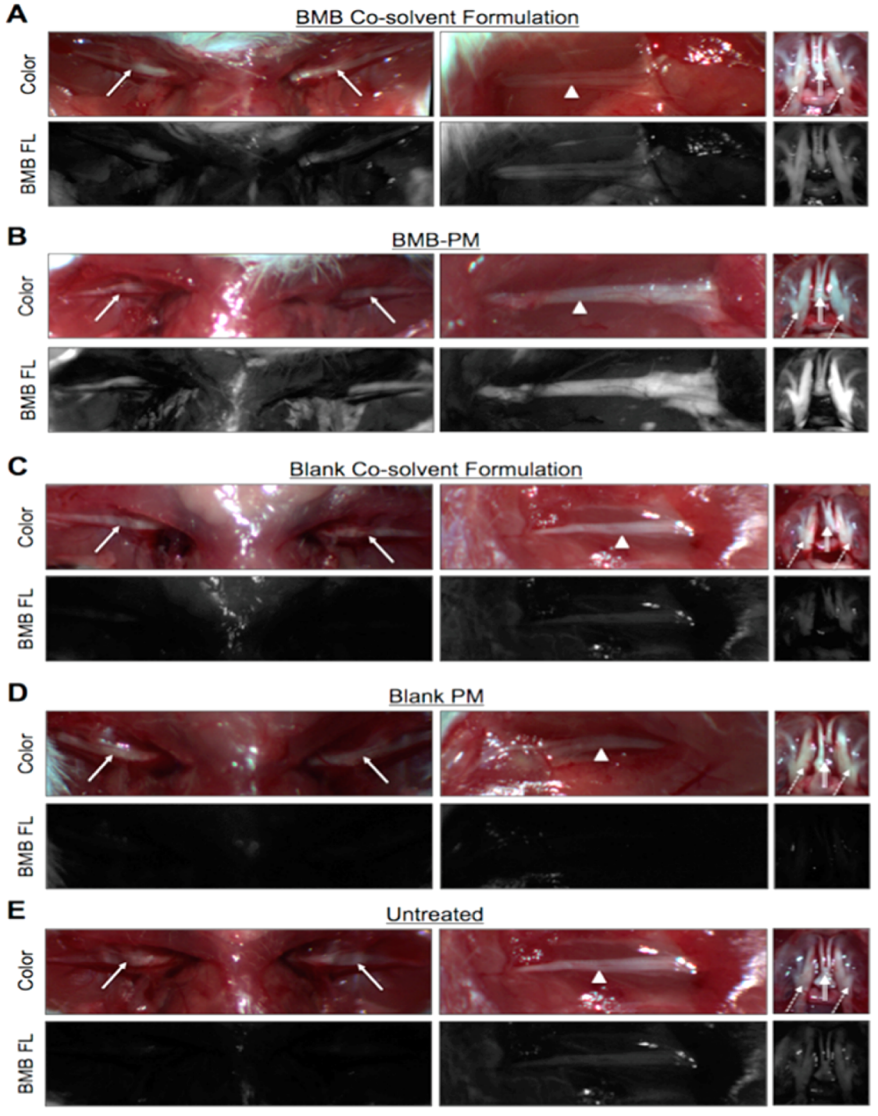

Figure 3. *In vivo* nerve-specific imaging of BMB-PM vs BMB in cosolvent. Representative color and fluorescence images (BMB FL) of mice administered 0.5 mg/kg BMB in (A) the cosolvent formulation or (B) BMB-PM. Representative color and fluorescence images of mice administered (C) blank cosolvent formulation and (D) blank PM. (E) Representative color and fluorescence images of untreated control mice. All images are representative of data collected for n = 3 mice per administration strategy. All fluorescence images were collected using 50 ms exposure time and are displayed with equal normalization. Brachial plexus = arrow, sciatic nerve = arrowhead, trigeminal ganglia = dashed arrow, optic nerve = double lined arrow.

10 μm tissue sections were cut onto Superfrost Plus slides. The tissue sections were washed once with PBS (2 min), fixed with 2% PFA (15 min), and then again washed with PBS (3 × 5 min). The tissue sections were incubated with BMB in the cosolvent formulation (n = 3) or BMB-PM (n = 3) at 100 μM for 20, 40, and 60 min at room temperature. A mixture of cosolvent formulation not containing BMB was used to wash the sections following fluorophore incubation (2 × 5 min) followed by additional washes with PBS (2 × 5 min). All stained slides were mounted using Fluoromount-G and imaged with the microscope

DOI: 10.1021/acs.molpharmaceut.5b00582
Mol. Pharmaceutics 2015, 12, 4386−4394

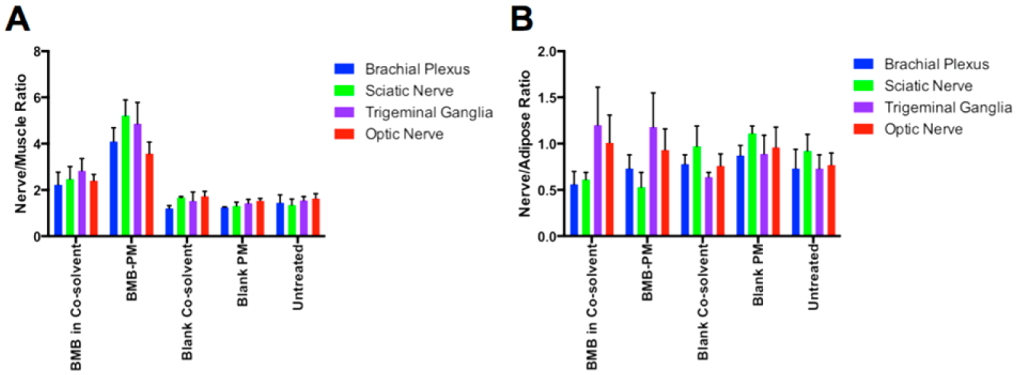

Figure 4. Nerve to muscle (N/M) and nerve to adipose ratio of BMB-PM vs BMB in cosolvent. (A) The mean nerve to muscle (N/M) ratio and standard deviation and (B) mean nerve to adipose (N/A) ratio and standard deviation were calculated using region of interest analysis for the brachial plexus, sciatic nerve, trigeminal ganglia, and optic nerves for each animal.

as described above. All images were acquired at 10 ms exposure time and displayed with equal normalization.

Statistical Analysis. Significant differences between treatment group means was evaluated using one-way ANOVA to compared all *in vivo* mean N/M and N/A ratios as well as the *ex vivo* mean nerve to background ratio from the resected tissues using GraphPad Prism. The means were compared between groups including BMB-PM, BMB in cosolvent, blank micelle, blank cosolvent, and untreated. Significant differences between the mean nerve to background ratio from the *ex vivo* nerve-specific staining using the BMB-PM vs the BMB in cosolvent were compared using unpaired two-sided *t* tests. All statistical analysis was performed with GraphPad Prism.

RESULTS

Micelle Encapsulation of Nerve-Specific Fluorophore and Release Kinetics. PEG-*b*-PLA PM were formulated and loaded with BMB. The BMB-PM micelles were able to solubilize BMB at 2.00 ± 0.55 mg/mL resulting in 100% loading efficiency. BMB-PM were stable at 25 °C for more than 30 days with more than 99% of the fluorophore retained in solution. BMB-PM were sized at 21.99 ± 0.06 nm (PDI = 0.113 ± 0.013). BMB-PM demonstrated unimodal distribution with PDI values of less than 0.2. BMB release from the BMB-PM micelles was assessed by dialysis in phosphate buffer over 72 h under sink conditions where 73.7% ± 2.6% of the fluorophore release occurred within 72 h (Figure 2A). Based on the two-phase exponential association curve fitting, the initial phase showed a rate constant of 1.93 h^{-1} and a half-life of 0.96 h while the second phase had a rate constant of 0.018 h^{-1} and a half-life of 38.77 h with an R^2 value of 0.9934. In addition we anticipate that the release *in vivo* would be significantly faster due to the presence of plasma proteins.[27]

Cell Viability Studies. The effect of the BMB-PM on cell viability was assessed in HUVEC and RAW 264.7 cells (Figures 2B and 2C). No significant effect on HUVEC cell viability was seen until a 1 μM concentration of BMB was achieved, while in RAW 264.7 cells there was no effect on cell viability until the BMB concentration of 100 μM was achieved. *In vivo* fluorophore concentrations reaching 100 μM are not anticipated due to the dynamic clearance mechanisms.

Murine Nerve Imaging. Previous dose and biodistribution studies using BMB demonstrated maximum N/M ratio 4 h after administration of 0.5 mg/kg BMB per mouse.[10] Mice were iv administered a 0.5 mg/kg dose of BMB in the cosolvent formulation (Figure 3A) or BMB-PM (Figure 3B). Four hours after iv fluorophore administration, the brachial plexus, sciatic nerve, trigeminal ganglia, and optic nerves were exposed for imaging. Color and fluorescence images of each nerve site were collected at 50 ms exposure time for equal comparison across nerve sites and formulations. Higher nerve fluorescence intensity was seen at all selected nerve sites for the BMB-PM as compared to BMB in the cosolvent (Figures 3A and 3B).

To determine if any tissue specific fluorescence signal was contributed by the formulations, mice were iv administered equivalent amounts of blank cosolvent formulation (Figure 3C) or blank PM (Figure 3D) 4 h prior to imaging. Autofluorescence at each of the nerve sites was also imaged on untreated control mice to quantify the contribution of tissue autofluorescence at the imaged wavelengths (Figure 3E). Minimal nerve autofluorescence was seen in the blank cosolvent formulation (Figure 3C), blank PM (Figure 3D), and untreated control mice (Figure 3E). Of note, nerve fluorescence was found to be nearly equivalent across the four nerve structures for control mice with blank PM, blank cosolvent, and untreated mice, demonstrating that neither formulation strategy contributed to nerve-specific fluorescence.

The N/M and N/A fluorescence ratios were quantified for each administration group at each nerve site including the brachial plexus, sciatic, trigeminal ganglia, and optic nerves. The N/M ratio was significantly higher at all nerve sites for the BMB-PM injected mice than for the BMB in cosolvent injected mice ($p < 0.0001$, Figure 4A). In the BMB-PM injected mice the N/M ratio was highest for the sciatic nerve (5.21 ± 0.68) followed by the trigeminal ganglia (4.86 ± 0.92), brachial plexus (4.10 ± 0.59), and optic nerves (3.57 ± 0.27). In the BMB in cosolvent injected mice the N/M ratio was highest for the trigeminal ganglia (2.83 ± 0.53), followed by the sciatic nerve (2.47 ± 0.54), optic nerve (2.40 ± 0.27), and brachial plexus (2.23 ± 0.54). When the N/M ratio was compared to average fluorescence intensity in the control blank PM, blank cosolvent, and untreated animals across nerve sites, the BMB-PM was 3× higher than control autofluorescence while the BMB in cosolvent was 1.7× higher than control autofluorescence (Figure 4A). Little fluorescence difference was seen between the three control groups with no statistically significant difference between the mean N/M fluorescence. The N/A fluorescence ratio was similar between the two formulation strategies ($p = 0.77$, Figure 4B). In both the BMB-PM and BMB in cosolvent the N/A ratio was highest in the trigeminal ganglia (BMB in cosolvent = 1.20 ± 0.41, BMB-PM = 1.18 ± 0.37) followed by the optic nerve (BMB in cosolvent = 1.01 ± 0.30, BMB-PM = 0.93 ± 0.23), brachial plexus (BMB in cosolvent = 0.56 ± 0.14, BMB-PM = 0.73 ±

DOI: 10.1021/acs.molpharmaceut.5b00582
Mol. Pharmaceutics 2015, 12, 4386−4394

0.15), and sciatic nerve (BMB in cosolvent = 0.61 ± 0.08, BMB-PM = 0.53 ± 0.16).

***Ex Vivo* Fluorescence Microscopy.** Following completion of the *in vivo* nerve imaging studies, all brachial plexus and sciatic nerve tissues were resected and flash frozen for *ex vivo* quantification by fluorescence microscopy. Representative phase contrast and fluorescence images of the brachial plexus and sciatic nerve tissues from mice administered BMB in the cosolvent formulation and BMB-PM as well as mice administered the blank cosolvent, blank PM, and untreated control are shown in Figure 5A. In untreated mice and blank controls a weak fluorescence background signal was seen in the nerve tissues, while significant nerve fluorescence was seen in the BMB injected animals. Fluorescence intensity was quantified in both the brachial plexus and sciatic nerves for each formulation group. Similar to the *in vivo* results, nerve to background fluorescence was significantly higher in the BMB-PM mice as compared to the BMB in the cosolvent injected mice ($p < 0.0001$) with little autofluorescence seen in the blank cosolvent, blank PM, or untreated control mouse nerve tissues (Figure 5B).

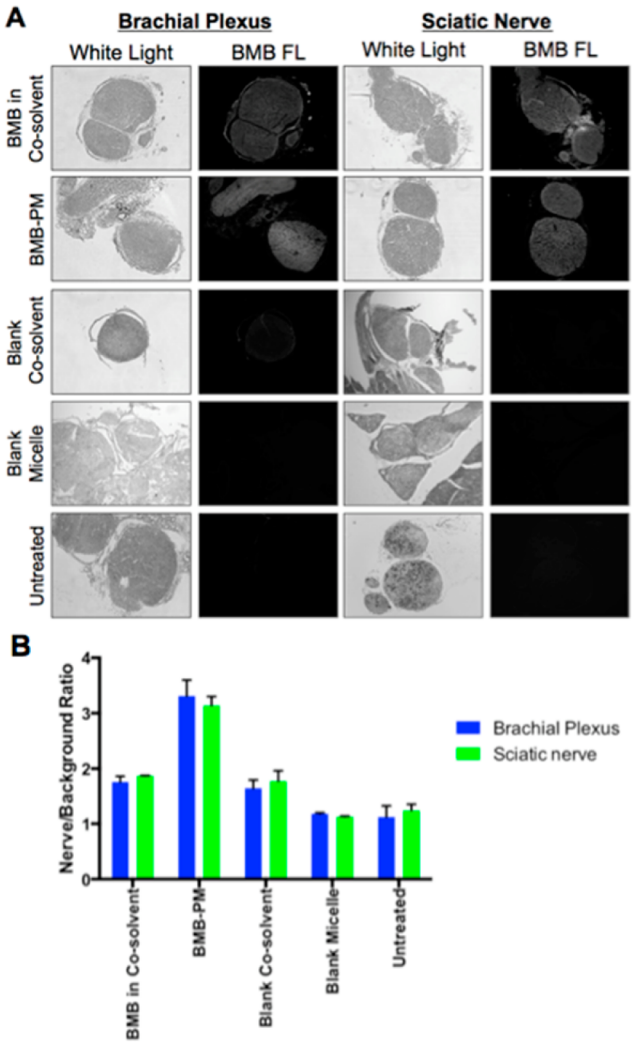

Figure 5. *Ex vivo* nerve-specific fluorescence of resected nerve tissues. All brachial plexus and sciatic nerve tissue was resected from $n = 3$ mice per administration group. (A) Representative white light and fluorescence images (BMB FL) of a brachial plexus and sciatic nerve from each administration group are shown. All fluorescence images were collected at 1000 ms exposure time and are displayed with equal normalization. (B) Nerve to background ratio was calculated for each mouse and for each formulation strategy. The average and standard deviation of the nerve to background ratio are shown for the brachial plexus and sciatic nerves.

***Ex Vivo* Nerve-Specific Staining of Micelle Encapsulated vs Cosolvent Formulated Fluorophore.** Brachial plexus and sciatic nerve tissue from untreated mice was used to examine the difference in fluorescence intensity following *ex vivo* BMB staining when BMB-PM or BMB in the cosolvent was used. Nerve tissues were stained using the previously developed *ex vivo* staining assay,[10,16] where the fluorophore incubation time was varied to include 20, 40, and 60 min to examine the effect of incubation time on the fluorescence intensity. Significantly greater nerve-specific fluorescence was seen using the BMB-PM as compared to BMB in the cosolvent in both the brachial plexus and sciatic nerve tissue sections ($p = 0.01$) as demonstrated by the lack of visible fluorescence in the BMB in cosolvent incubated slides when images were acquired with the same exposure time and displayed with equal normalizations (Figures 6A and 6B). Nerve to background ratio was quantified for both nerves at each incubation time and found to linearly increase with incubation time for both formulations (Figures 6C and 6D). The nerve to background ratio was 5−10× greater for the BMB-PM as compared to BMB in the cosolvent formulation at all three incubation times.

DISCUSSION

Nerve damage is a major morbidity experienced by patients that undergo numerous surgical procedures. This difficulty stems from the nature of the nerve tissue, which is generally small and translucent as well as the fact that nerves are typically protected deep within layers of surrounding tissue making them difficult to detect and visualize prior to injury or transection in surgery. Currently no clinically available imaging tool exists to enhance nerve visualization in the operating room. With the increased focus on fluorescence image-guided surgery as well as the approval of a select few imaging systems for clinical use, there is an opportunity to improve nerve visualization though fluorescence imaging in the surgical suite. However, few nerve-specific fluorescent contrast agents exist and, given the lipophilic nature of nerve tissue, systemic administration of these agents has proven challenging. To date, two select small molecule fluorophore scaffolds have been demonstrated to provide nerve-specific fluorescence in all nerve tissue following systemic administration in a cosolvent formulation that is not suited for clinical translation due to its potential toxicity and reliance on DMSO, which is not FDA approved.[10,16,17,28] Development of a formulation strategy with the potential for nontoxic clinical translation would significantly improve the prospects of using specific probes from either of these nerve-specific fluorophore scaffold families for fluorescent nerve-specific image-guided surgery.

In the current work, the previously used DMSO containing cosolvent formulation was compared to a nontoxic PM formulation *in vivo* and *ex vivo* to assess the effect of formulation strategy on nerve-specific fluorophore accumulation. The previously characterized cosolvent formulation containing Cremophore EL and DMSO is capable of solubilizing BMB at 5 mg/mL but is not a viable clinical option for surgical use.[28] BMB-PM was formulated in a biodegradable, biocompatible polymer, which has an extensively documented safety profile in humans.[20,23] The *in vitro* release profile of BMB from the polymeric micelles (Figure 2A) and the curve fitting analysis

DOI: 10.1021/acs.molpharmaceut.5b00582
Mol. Pharmaceutics 2015, 12, 4386−4394

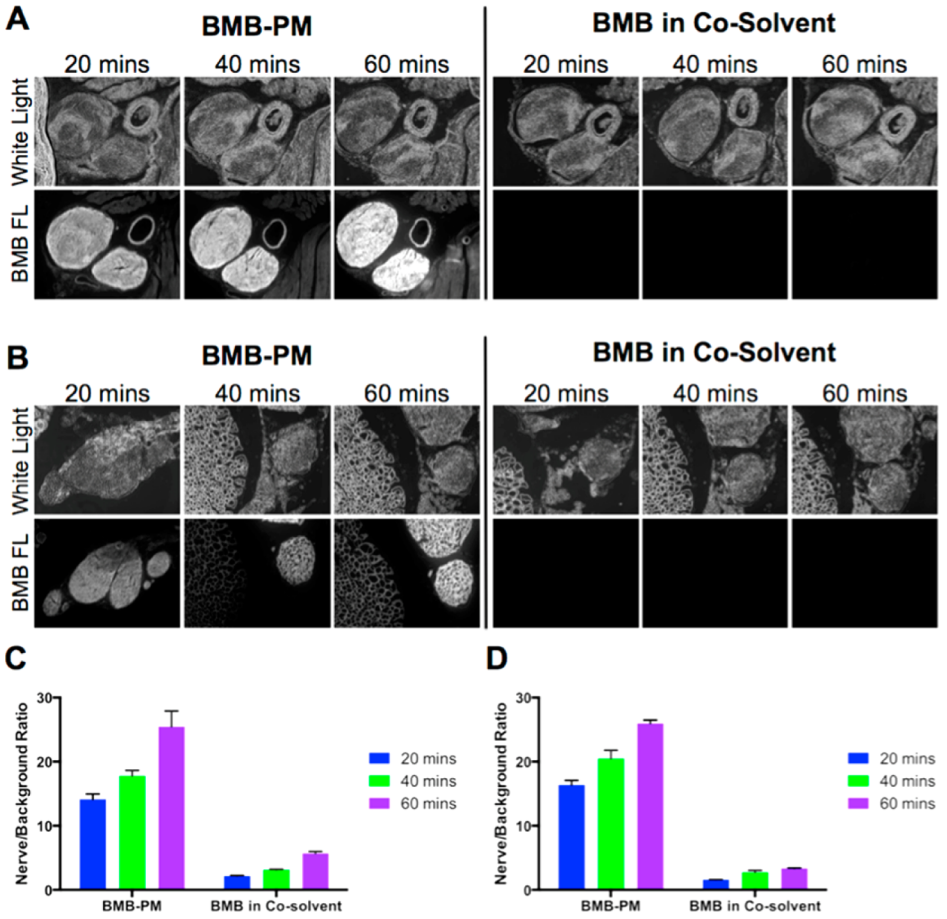

Figure 6. *Ex vivo* nerve-specific staining. Resected unstained mouse (A) brachial plexus and (B) sciatic nerve tissue was stained using 100 μM micelle encapsulated or cosolvent formulated BMB. Nerve sections were incubated with BMB for 20, 40, or 60 min. White light and fluorescence images (BMB FL) were collected. All fluorescence images were collected at 10 ms exposure time and are displayed with equal normalization. Nerve to background ratio was calculated for the micelle encapsulation vs the cosolvent formulation incubated for 20, 40, or 60 min on the (C) brachial plexus or (D) sciatic nerve tissue sections.

showed that BMB release from the polymeric micelles was biphasic, where the initial phase involved a rapid release of BMB followed by a sustained release pattern at the longer time points. This biphasic release pattern exhibited by polymeric micelles and nanoparticales demonstrated herein has been well documented in the literature.[29,30] The initial rapid release of BMB was primarily driven by the desorption and diffusion of surface adsorbed fluorophore, while the secondary phase of fluorophore release was driven by the dissociation of the polymeric matrix and fluorophore diffusion process. *In vitro* cell viability assessment in the presence of BMB-PM in two primary cell lines indicated that no effect on viability was seen below 100 μM depending on the sensitivity of the cells (Figures 2B and 2C). Systemic administration of the BMB-PM for *in vivo* study is at a lower concentration, thus the accumulated concentration in any one cell is less than the determined toxic dose of the BMB-PM formulation. Consequently, we do not anticipate systemic toxicity *in vivo* due to the dynamic nature of clearance mechanisms and the unlikelihood of a tissue being exposed to toxic levels of BMB-PM concentrations prior to clearance from the body. Therefore, the BMB-PM formulation offers a safer and more effective alternative to the previously utilized cosolvent system.

In addition to its improved safety profiles, the BMB-PM significantly improved nerve-specific accumulation of the fluorophores. *In vivo* studies comparing BMB-PM and BMB in the cosolvent demonstrated increased nerve-specific fluorescence in the BMB-PM group following administration of the same dose of fluorophore in both formulations (Figures 3 and 4). Interestingly the nerve fluorescence was greatly increased in the BMB-PM injected animals as compared to the BMB in cosolvent injected animals while the muscle fluorescence remained largely the same in both cohorts, accounting for the increased N/M ratio in the BMB-PM group. By comparison the adipose fluorescence also increased in the BMB-PM injected animals, thus the N/A ratio was found to be similar between the BMB-PM and BMB in cosolvent injected groups. Although the PM formulation strategy did not improve the N/A ratio, it did not significantly alter it from what was seen in the BMB in cosolvent administered group. The adipose accumulation seen using both formulation strategies likely has little to do with the formulation strategy itself and is rather a property of the fluorophore, which has a lipophilic Log *D* (Log *D* = 4.8 at pH 7.4) accounting for the adipose accumulation. By comparison the BMB-PM demonstrated 3× the N/M contrast over control tissue autofluorescence while the BMB in cosolvent had only 1.7× the N/M contrast over control tissue. This increase in nerve-specific fluorophore accumulation may stem from a potentially longer blood circulation time of the fluorophore when PM encapsulated vs solubilized in the cosolvent. Thus, overall the N/M fluorescence was significantly

DOI: 10.1021/acs.molpharmaceut.5b00582
Mol. Pharmaceutics 2015, 12, 4386−4394

increased in the BMB-PM group as compared to BMB in the cosolvent group ($p < 0.0001$) without an increase in fluorophore dose (Figure 4). Future studies will be performed to evaluate the effect of BMB polymeric micelle encapsulation on blood circulation, biodistribution, and pharmacokinetic differences of BMB nerve accumulation, which will provide additional insight into BMB stability and distribution in the body.

As expected, when the resected nerve tissue was examined microscopically, nerve to background fluorescence was significantly higher in the BMB-PM group as compared to BMB in the cosolvent group ($p < 0.0001$, Figure 5). Of note, when *ex vivo* staining was performed, a linear increase in fluorescence intensity was seen in both the BMB-PM and BMB in cosolvent groups, however the fluorescence intensity of the BMB-PM group was significantly greater than that of the BMB in cosolvent group ($p = 0.01$, Figure 6). Again a possible explanation for this observation is improved availability of the fluorophore to the nerve tissue through improved solubility using the PM over the cosolvent formulation which was demonstrated both in the blood (*in vivo*) and in solution (*ex vivo* staining study).

In summary, a micellar formulation for BMB has been successfully developed and characterized improving the feasibility of clinical translation of this nerve specific fluorophore for fluorescence image-guided surgery through an improved safety profile. Another attractive feature of the PM formulation strategy for clinical translation is the enhanced N/M ratio following administration of BMB-PM as compared to BMB in the cosolvent formulation without increasing fluorophore dose, an important consideration for clinical safety. The increase in N/M ratio provides the opportunity to lower fluorophore dose while creating equivalent N/M ratio of that seen with the cosolvent formulation, further improving the safety profile. Future work lies in scaling up the formulation, studies in a larger animal model such as swine, translation of the formulation strategy to other promising nerve-specific fluorophores within the two known nerve-specific families, and fully characterizing the formulation for complete preclinical assessment.

AUTHOR INFORMATION

Corresponding Author

*Oregon Health & Science University, Collaborative Life Sciences Building, 2730 SW Moody Ave., Mail Code CL3SG, Portland, OR 97201. E-mail: gibbss@ohsu.edu. Phone: 503-494-8940.

Author Contributions

‡K.M.H. and B.S.D. contributed equally to this work.

Notes

The authors declare no competing financial interest.

ACKNOWLEDGMENTS

We would like to thank Brandon Lei for experiment assistance. This study was supported by grants from the National Institutes of Health NIBIB K01EB010201 (S.L.G.), the Oregon Clinical and Translational Research Institute (S.L.G.) at Oregon Health and Science University, and Oregon State University Start-up Funding (A.W.G.A.).

REFERENCES

(1) Burke, S.; Shorten, G. D. When pain after surgery doesn't go away. *Biochem. Soc. Trans.* **2009**, *37*, 318−322.

(2) Keereweer, S.; et al. Optical image-guided surgery–where do we stand? *Molecular imaging and biology: MIB: the official publication of the Academy of Molecular Imaging* **2011**, *13*, 199−207.

(3) Frangioni, J. V. New technologies for human cancer imaging. *J. Clin. Oncol.* **2008**, *26*, 4012−4021.

(4) van Dam, G. M.; et al. Intraoperative tumor-specific fluorescence imaging in ovarian cancer by folate receptor-alpha targeting: first in-human results. *Nat. Med.* **2011**, *17*, 1315−1319.

(5) Gioux, S.; Choi, H. S.; Frangioni, J. V. Image-guided surgery using invisible near-infrared light: fundamentals of clinical translation. *Mol. Imaging* **2010**, *9*, 237−255.

(6) Ntziachristos, V.; Yoo, J. S.; van Dam, G. M. Current concepts and future perspectives on surgical optical imaging in cancer. *J. Biomed. Opt.* **2010**, *15*, 066024.

(7) Gibbs, S. L. Near infrared fluorescence for image-guided surgery. *Quant. Imaging Med. Surg.* **2012**, *2*, 177−187.

(8) Vahrmeijer, A. L.; Hutteman, M.; van der Vorst, J. R.; van de Velde, C. J.; Frangioni, J. V. Image-guided cancer surgery using near-infrared fluorescence. *Nat. Rev. Clin. Oncol.* **2013**, *10*, 507−518.

(9) Keereweer, S.; et al. Optical image-guided cancer surgery: challenges and limitations. *Clin. Cancer Res.* **2013**, *19*, 3745−3754.

(10) Gibbs-Strauss, S. L.; et al. Nerve-highlighting fluorescent contrast agents for image-guided surgery. *Mol. Imaging* **2011**, *10*, 91−101.

(11) Whitney, M. A.; et al. Fluorescent peptides highlight peripheral nerves during surgery in mice. *Nat. Biotechnol.* **2011**, *29*, 352−356.

(12) Wang, C.; et al. In situ fluorescence imaging of myelination. *J. Histochem. Cytochem.* **2010**, *58*, 611−621.

(13) Wang, C.; et al. Longitudinal near-infrared imaging of myelination. *J. Neurosci.* **2011**, *31*, 2382−2390.

(14) Wu, C.; et al. Molecular probes for imaging myelinated white matter in CNS. *J. Med. Chem.* **2008**, *51*, 6682−6688.

(15) Gibbs-Strauss, S. L.; et al. Molecular imaging agents specific for the annulus fibrosus of the intervertebral disk. *Mol. Imaging* **2010**, *9*, 128−140.

(16) Gibbs, S. L.; et al. Structure-activity relationship of nerve-highlighting fluorophores. *PLoS One* **2013**, *8*, e73493.

(17) Park, M. H.; et al. Prototype nerve-specific near-infrared fluorophores. *Theranostics* **2014**, *4*, 823−833.

(18) ACD/Labs in Advanced Chemistry Development, Edn. Version 14.0.0 (ACD/Labs, Toronto, Ontario, Canada; 2014).

(19) Dong, H.; et al. Long-circulating 15 nm micelles based on amphiphilic 3-helix peptide-PEG conjugates. *ACS Nano* **2012**, *6*, 5320−5329.

(20) Kwon, G. S. Polymeric micelles for delivery of poorly water-soluble compounds. *Crit. Rev. Ther. Drug Carrier Syst.* **2003**, *20*, 357−403.

(21) Mishra, G. P.; Nguyen, D.; Alani, A. W. Inhibitory effect of paclitaxel and rapamycin individual and dual drug-loaded polymeric micelles in the angiogenic cascade. *Mol. Pharmaceutics* **2013**, *10*, 2071−2078.

(22) Torchilin, V. P. Structure and design of polymeric surfactant-based drug delivery systems. *J. Controlled Release* **2001**, *73*, 137−172.

(23) Adams, M. L.; Lavasanifar, A.; Kwon, G. S. Amphiphilic block copolymers for drug delivery. *J. Pharm. Sci.* **2003**, *92*, 1343−1355.

(24) Lu, Y.; Park, K. Polymeric micelles and alternative nanonized delivery vehicles for poorly soluble drugs. *Int. J. Pharm.* **2013**, *453*, 198−214.

(25) Mishra, G. P.; Doddapaneni, B. S.; Nguyen, D.; Alani, A. W. Antiangiogenic effect of docetaxel and everolimus as individual and dual-drug-loaded micellar nanocarriers. *Pharm. Res.* **2014**, *31*, 660−669.

(26) Ahn, H. K.; et al. A phase II trial of Cremorphor EL-free paclitaxel (Genexol-PM) and gemcitabine in patients with advanced non-small cell lung cancer. *Cancer Chemother. Pharmacol.* **2014**, *74*, 277−282.

(27) Lu, J.; Owen, S. C.; Shoichet, M. S. Stability of Self-Assembled Polymeric Micelles in Serum. *Macromolecules* **2011**, *44*, 6002−6008.

(28) Montaguti, P.; Melloni, E.; Cavalletti, E. Acute intravenous toxicity of dimethyl sulfoxide, polyethylene glycol 400, dimethylformamide, absolute ethanol, and benzyl alcohol in inbred mouse strains. *Arzneim.-Forsch.* **1994**, *44*, 566−570.

DOI: 10.1021/acs.molpharmaceut.5b00582
Mol. Pharmaceutics 2015, 12, 4386−4394

(29) Li, R.; et al. Preparation and evaluation of PEG-PCL nanoparticles for local tetradrine delivery. *Int. J. Pharm.* **2009**, *379*, 158−166.
(30) Peng, W.; et al. Oral delivery of capsaicin using MPEG-PCL nanoparticles. *Acta Pharmacol. Sin.* **2015**, *36*, 139−148.

DOI: 10.1021/acs.molpharmaceut.5b00582
Mol. Pharmaceutics 2015, 12, 4386−4394